

We are IntechOpen, the world's leading publisher of Open Access books Built by scientists, for scientists

6,900

Open access books available

185,000

International authors and editors

200M

Downloads

Our authors are among the

154

Countries delivered to

TOP 1%

most cited scientists

12.2%

Contributors from top 500 universities



WEB OF SCIENCE™

Selection of our books indexed in the Book Citation Index
in Web of Science™ Core Collection (BKCI)

Interested in publishing with us?
Contact book.department@intechopen.com

Numbers displayed above are based on latest data collected.
For more information visit www.intechopen.com



Application of Probe Nanotechnologies for Memristor Structures Formation and Characterization

*Vladimir A. Smirnov, Marina V. Il'ina, Vadim I. Avilov,
Roman V. Tominov, Oleg I. Il'in and Oleg A. Ageev*

Abstract

This chapter presents the results of experimental studies of the formation and investigation of the memristors by probe nanotechnologies. This chapter also perspectives and possibilities of application of local anodic oxidation and scratching probe nanolithography for the manufacture of memristors based on titanium oxide structures, nanocrystalline ZnO thin film, and vertically aligned carbon nanotubes. Memristive properties of vertically aligned carbon nanotubes, titanium oxide, and ZnO nanostructures were investigated by scanning probe microscopy methods. It is shown that nanocrystalline ZnO films manifest a stable memristor effect slightly dependent on its morphology. Titanium oxide nanoscale structures of different thicknesses obtained by local anodic oxidation demonstrate a memristive effect without the need to perform any additional electroforming operations. This experimentally confirmed the memristive switching of a two-electrode structure based on a vertically aligned carbon nanotube. These results can be used in the development of designs and technological processes of resistive random access memory (ReRAM) units based on the memristor devices.

Keywords: nanotechnology, scanning probe microscopy, memristor, titanium oxide, nanocrystalline ZnO films, carbon nanotubes

1. Introduction

Reducing the elements of integrated circuits (ICs) leads to an increase in the speed of the processors and an increase in the amount of memory, but at the same time the bandwidth between them varies only slightly. This is referred as the von Neumann bottleneck and often limits the performance of the system [1]. One possible solution to this problem is the transition of computing systems to an architecture close to the structure of a biological brain, which is a set of elements of low power connected in parallel neurons interconnected via special channels synapses [1–4]. Processors built on this architecture have concurrent computing and will be able to surpass modern computers in tasks related to unstructured data classification, pattern recognition, as well as in applications with adaptable and self-learning

control systems. One of the possible ways of implementing such an architecture is to manufacture ICs based on neuromorphic structures, which are memory elements in the form of cells (neurons) interconnected by data buses (synapses) and are capable of changing their electrical resistance under the influence of an external electric field (the effect of resistive switch) [1–5]. Such structures can maintain cell resistance after the termination of the external electric field and are the basis of non-volatile resistive memory (ReRAM). The advantages of ReRAM include small size, high degree of integration, low power consumption, and high speed, which allows on its basis to realize the mass parallelism and low power calculations observed in the study of biological brain [6–8].

Currently, active theoretical and experimental studies of the effect of resistive switching in nanomaterials and nanostructures are underway to create elements of the ReRAM self-learning adaptive neuromorphic processor with high speed and low power consumption. An analysis of the publications showed that for the manufacture of ReRAM, films based on binary metal oxides (SiO_x , TiO_2 , ZnO , HfO_x , etc.) are promising from which amorphous titanium oxide and nanocrystalline zinc oxide can be distinguished, allowing for high response speed of the resistive switching process [8–10].

The creation of ReRAM elements for a neuromorphic processor is associated with the development and research of the formation processes of structures with a nanometer resolution. Existing lithographic methods of semiconductor technologies are approaching the limit of their resolution, characterized by a high degree of complexity and cost of equipment. Therefore, there is a need for research and development of new methods, the use of which will allow the creation of nanostructures of ReRAM elements, including at the prototyping stage.

One possible way of ReRAM elements prototyping is probe nanotechnologies usage, which is a combination of methods for nanostructures forming using a probe tip with visualization and process control in situ. Promising methods of probe nanotechnologies for ReRAM elements prototyping include local anodic oxidation (LAO) and scanning probe nanolithography (SPN) of atomic force microscope.

The method of local anodic oxidation is promising for the manufacture of oxide nanostructures (ONS) of titanium, which have reproducible memristor effect and do not require forming [11–14]. The advantages of the LAO method also include precision, the possibility of conducting research on electrochemical processes in local areas up to the size of several nanometers in situ diagnostics of the results of the formation of ONS on the substrate surface, the absence of additional technological operations for applying, exposing, and removing photoresist, as well as the relatively low cost of process equipment [15–20]. A variety of nanoimprint lithography is scratching probe nanolithography, which allows using the tip of an atomic force microscope probe to form profiled nanostructures in polymer films [21]. The simplicity of the method implementation allows using it in the development and study of promising design and technological solutions for prototyping ReRAM elements [22].

At the present stage of nanotechnology development, one of the most promising methods for surface diagnostics is scanning probe microscopy (SPM). The use of SPM methods allows the study of the local geometric, electrical, and mechanical properties of the sample surface [23–26].

Of interest for creating ReRAM with high cell density are memristor structures based on vertically aligned carbon nanotubes (VA CNTs) [27, 28]. The vertical orientation of the nanotubes provides a significant reduction in the memory cell area and the technology of producing VA CNTs based on the method of plasma-enhanced chemical vapor deposition (PECVD) allows localized growth of nanotubes in a process compatible with silicon technology [29, 30]. In addition, the use of VA CNTs as a storage element is expected to reduce the switching time to picoseconds [28, 31].

A promising method of probe nanotechnologies for creation and characterization of memristor structures based on VA CNTs is the scanning tunneling microscopy (STM) [26]. This method allows you to create a controlled elastic deformation in VA CNT, the presence of which is a prerequisite for the occurrence of the memristor effect in VA CNT [32]. The mechanism of memristive switching of strained carbon nanotube is described in detail in [28].

This chapter describes application of scanning probe microscopy techniques for determination of resistive switching effects in vertically aligned carbon nanotubes, TiO₂ nanostructures, and ZnO thin nanocrystalline films. Described techniques can be used for formation and nanodiagnostics of parameters of memristor structures for creation of metal oxide and CNT-based neuromorphic system.

2. Formation and investigation of memristor structures based on titanium oxide by atomic force microscopy

2.1 Investigation of resistive switching of titanium oxide nanostructures formed by local anodic oxidation

The memristor effect study was carried out on titanium oxide nanostructures (ONS) using AFM spectroscopy using SPM Solver P47 Pro. For this purpose, local anodic oxidation (LAO) was carried out on the thin titanium film surface with a 20 nm thickness, and as a result, titanium ONS was formed with lateral dimensions $1 \times 1 \mu\text{m}$ and 1.1 nm thick (**Figure 1**).

Then, using the AFM, the current-voltage (I-V) characteristics of the obtained structure were measured according to the scheme shown in **Figure 1c** with the application of a triangular-shaped voltage pulse (**Figure 2a** inset). It was shown that the titanium ONS obtained by the LAO exhibits a bipolar resistive switching effect (**Figure 2**) without additional doping and electroforming operations.

The analysis showed that the current-voltage characteristic type corresponds to the switching mechanism due to potential barrier width modulation at the

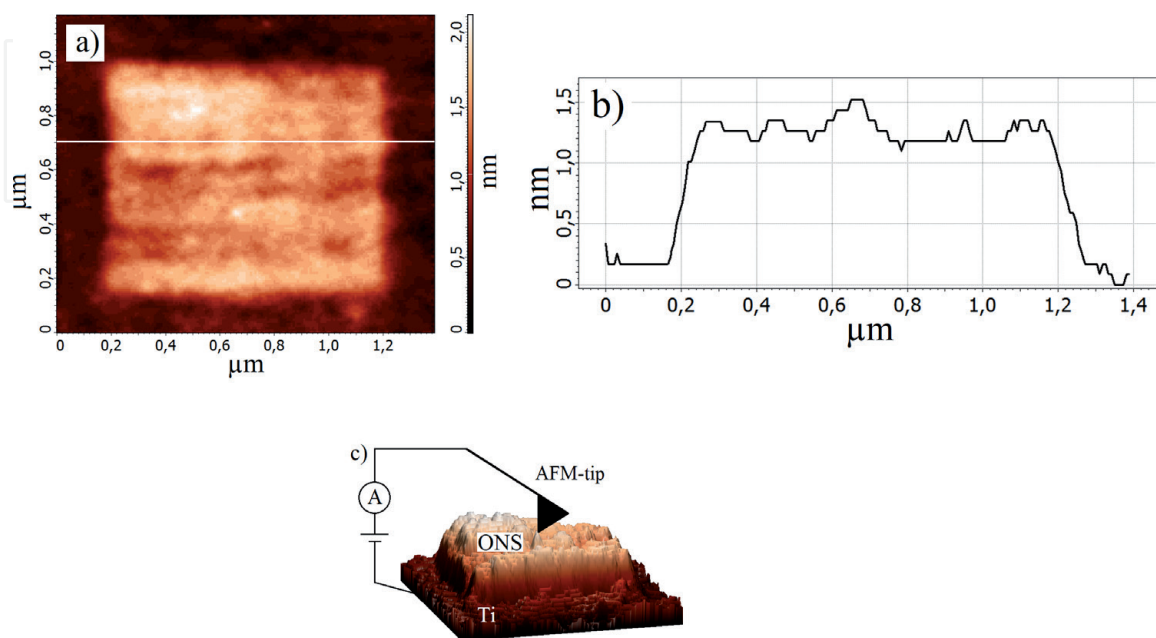


Figure 1. Titanium oxide nanostructures, formed by LAO: (a) AFM image; (b) profilogram along the line; and (c) current-voltage characteristics measuring scheme.

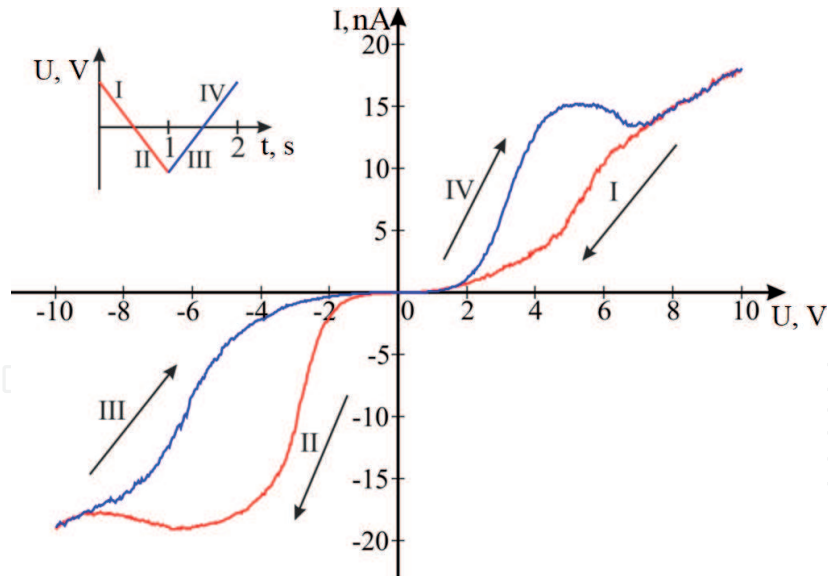


Figure 2.
Current-voltage characteristic of titanium ONS, formed by the LAO.

electrode/oxide interface described in [11, 12]. In this case, the potential barrier modulation occurs alternately at both the electrodes boundaries.

Initially, the structure is in high resistance state (HRS) ($1.3 \text{ G}\Omega$ at 3.5 V) in the forward bias region (region I in **Figure 2**), while at a negative voltage applied to -5 V , the structure is in low resistance state (LRS) ($0.27 \text{ G}\Omega$ at -3 V) (region II in **Figure 2**). Then, as the voltage rises in the reverse bias region from -6 to -10 V , the structure is switched, resulting in a HRS state ($3.4 \text{ G}\Omega$ at -3 V) at the reverse bias (region III in **Figure 2**) and LRS ($0.35 \text{ G}\Omega$ at 3.5 V) at up to 5 V direct bias (region IV in **Figure 2**). With an increase in the applied voltage from 6 to 10 V , the structure is switched to the initial state. In this case, the structure resistance ratio in the HRS state to the LRS state for positive voltages is 3.6 , and for negative voltages is 12.6 .

2.2 Investigation of influence of AFM probe pressing force on the resistive switching in titanium oxide nanostructures

For the experimental study, titanium ONS with $2 \times 2 \text{ }\mu\text{m}$ lateral dimensions and 6.8 nm thick was formed by LAO. Then, on its surface in the AFM contact mode was performed a spectroscopic measurement of dependence of the feedback circuit current on the cantilever beam bending. The spectrogram showed that with an increase in the feedback circuit current by 1.02 nA , the beam is bent by 20.8 nm . Since the cantilever beam stiffness is 2.5 N/m , it is possible to calculate the AFM probe pressing force to the ONS surface for a given feedback circuit current **Figure 3**.

Then, current-voltage characteristics were measured on the ONS surface in the $\pm 10 \text{ V}$ range with the AFM feedback circuit current values from 0.01 to 2 nA (**Figure 4**), after which the structure resistance values in the HRS and LRS states were measured at 3.5 V .

Obtained dependences analysis showed that an increase in the AFM probe clamping force to the surface from 0.51 to 102.8 nN leads to a decrease in the structure resistance in the HRS state from 1.12×10^{11} to $9.63 \times 10^9 \text{ }\Omega$ and in the LRS state from 2.28×10^{10} to $1.38 \times 10^9 \text{ }\Omega$.

This dependence can be explained by the fact that with a clamping force increase, an increase in the contact area between the AFM probe and the oxide

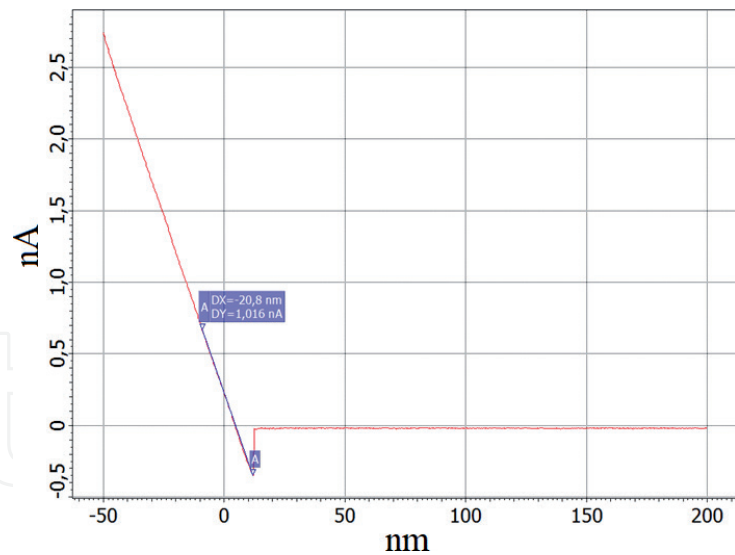


Figure 3.
Dependence of feedback circuit current from the cantilever beam bending.

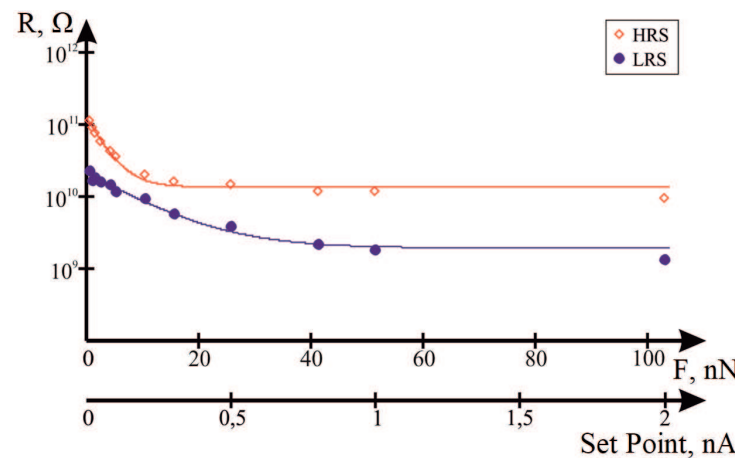


Figure 4.
Dependence of titanium ONS resistance in the HRS and LRS states on the pressing force.

surface occurs. In further studies, 60 nN clamping force was used, ensuring reliable contact of the probe with the structure.

2.3 Investigation of influence of top electrode materials on the resistive switching in titanium oxide nanostructures

Literature analysis showed that the top electrode material has a significant impact on the resistive switching of memristor structures. To study this effect, the current-voltage characteristics were measured in the mode of current AFM spectroscopy on the surface of oxide nanostructures formed by the LAO method; AFM probes with different conducting coating were used as the upper electrode. The resulting characteristics are presented on (Figure 5).

Obtained dependences analysis showed that the use of cantilevers with different coatings significantly affects the manifested memristor effect. So, when using a cantilever with a Pt coating, a symmetrical I-V characteristic was obtained (Figure 5a) with low current values, the structure resistance in the HRS state is $327 \times 10^9 \Omega$, and in the LRS state is $22 \times 10^9 \Omega$, while the resistance ratio in the high resistance to low resistance is 15.

When using a cantilever with a TiN coating, an asymmetric I-V characteristic was obtained (Figure 5b), while in the negative voltage region the memristor effect

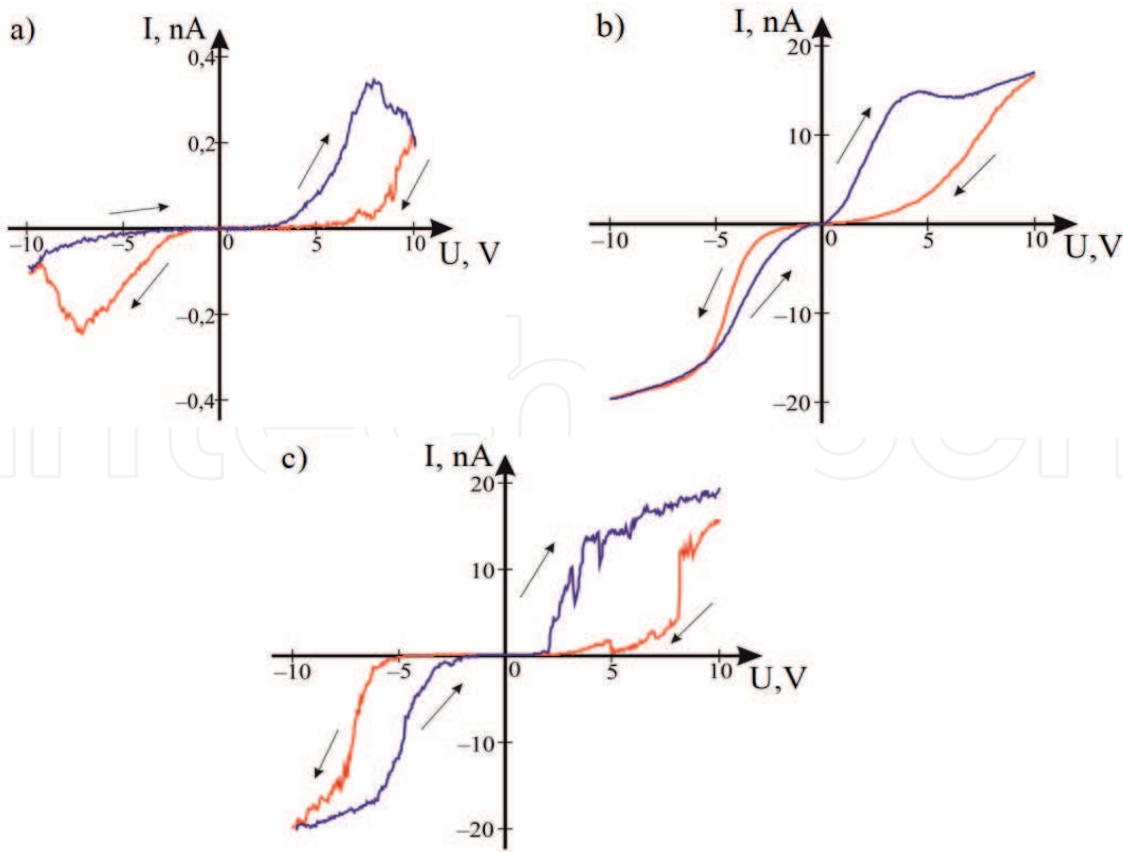


Figure 5. Titanium ONS current-voltage characteristics, obtained using a cantilever coated by: (a) Pt; (b) TiN; and (c) carbon.

is insignificant, the structure's resistance in the HRS state is $4.65 \times 10^9 \Omega$, and in the LRS state $-0.39 \times 10^9 \Omega$, at the same time, resistance ratio in the high resistance to low resistance is 12. In the case of using a carbon-coated cantilever, an asymmetric I-V characteristic is also observed (**Figure 5c**), and there is no current through the ONS when applying voltages less than ± 5 V in the case of a structure being in HRS and applying a voltage less than ± 2 V in case of a structure being in LRS. The structure's resistance in the HRS state is $1.74 \times 10^9 \Omega$, and in the LRS state, it is $0.3 \times 10^9 \Omega$, and the resistance ratio in the high resistance to low resistance is 6.

Study results showed that the platinum-coated cantilever use as the top electrode is characterized by a largest resistance ratio in the HRS and LRS states.

2.4 Investigation of influence of titanium oxide nanostructures geometric parameters on their resistive switching

Another goal is to study titanium ONS thickness effect and applied voltage pulses on the memristor effect. For this, four ONSs were formed with lateral $2 \times 2 \mu\text{m}$ dimensions and 1.6–3.6 nm height, which, based on the expression describing the oxide height and depth ratio presented in [3], corresponds to 3.6–8.2 nm thickness. The current-voltage characteristics were measured on these structures surface by applying ± 2.4 voltage pulse (**Figure 6**).

Obtained expression analysis showed that with an increase in the ONS thickness, a decrease in the current corresponding to the LRS state and an increase in the resistance in this state are observed, to the extent that the memristor effect does not manifest itself when the oxide thickness is 8.2 nm.

The results allowed us to obtain voltage of the switching structure in the HRS state (U_{res}) and in the LRS state (U_{set}) dependence, as well as the corresponding

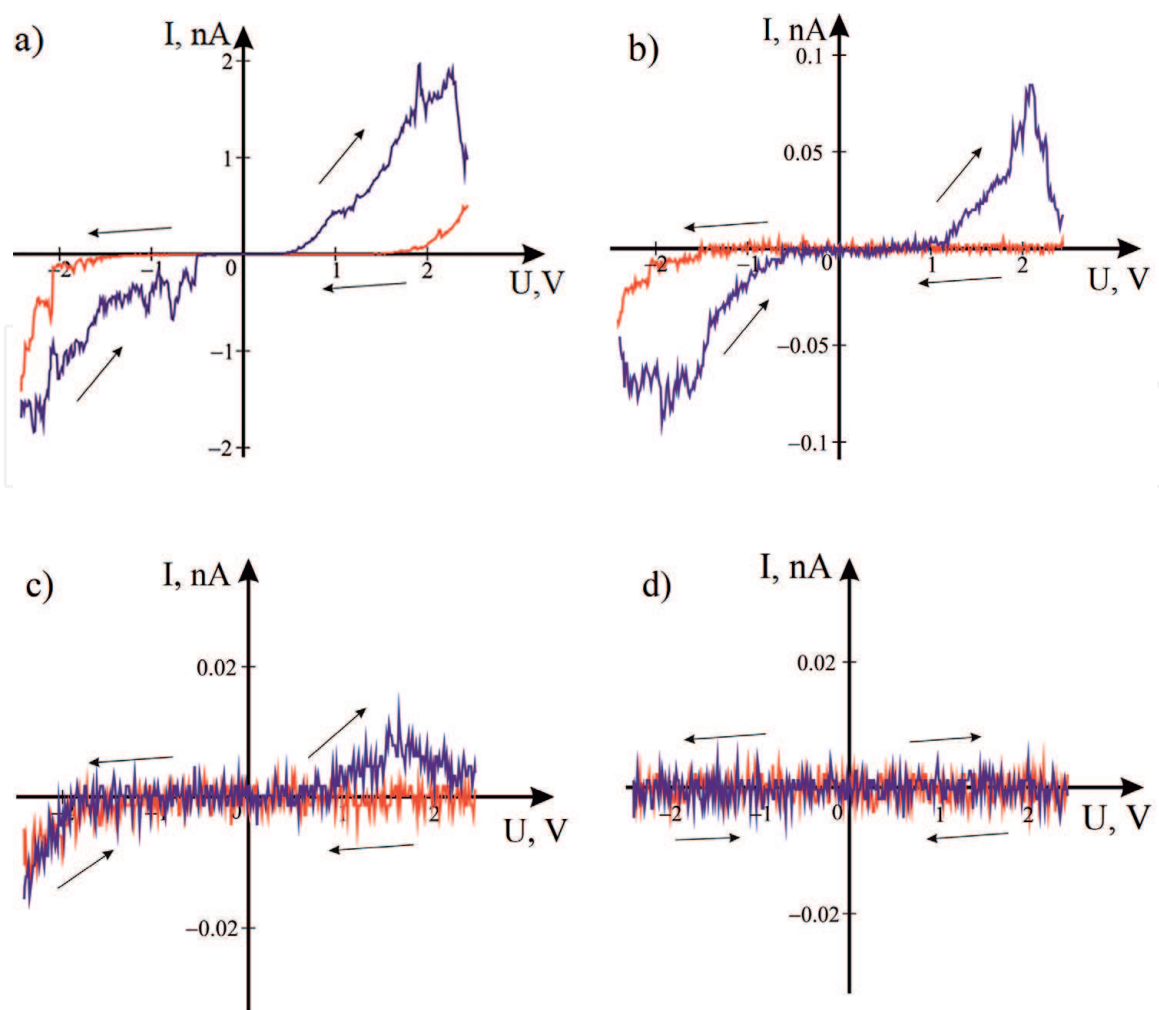


Figure 6.
 Titanium ONS current-voltage characteristics with a thickness: (a) 3.6 nm; (b) 5.4 nm; (c) 7.2 nm; and (d) 8.2 nm.

currents (I_{res} and I_{set}) on the titanium ONS thickness (**Figure 7**). In addition, the dependence of the structure resistance measured in a HRS and LRS state on the ONS thickness measured at 1.5 V was obtained (**Figure 8**).

It is shown that increasing the thickness from 3.6 to 8.2 nm increases the resistance in the HRS state from 1.4×10^{11} to $8.8 \times 10^{11} \Omega$, while the resistance in the LRS state increases from 1.765×10^9 to $2.4 \times 10^{11} \Omega$, while the structure resistance ratio in the high resistance to low resistance decreases from 79.4 to 3.6.

2.5 Investigation of influence of voltage pulses amplitude on the titanium oxide nanostructures resistive switching

To study the applied voltage pulses amplitude effect on the memristor effect, an titanium ONS with $2 \times 2 \mu\text{m}$ lateral dimensions and 3.6 nm thickness was formed. Then, its current-voltage characteristic was measured in the voltage range from ± 1 to ± 4 V (**Figure 9**).

The analysis showed that when measuring the titanium ONS current-voltage characteristics with 3.6 nm thickness in the voltage range ± 1 V, the memristor effect is not observed, the structure shows the conductivity absence. When measuring the I-V characteristic in the ± 2 V range, the structure also shows the conductivity absence, however, a small current surge in the I-V characteristic is already observed. When measuring the I-V characteristic in ± 3 and ± 4 V range, this structure exhibits a memristor effect. It is shown that in the case of measuring the I-V characteristic in ± 3 V range, the structure resistance in the HRS state is $39.2 \times 10^9 \Omega$, and in the LRS

state $-1.4 \times 10^9 \Omega$, the resistance ratio in the HRS and LRS states is 27.4. In the case of measuring the I-V characteristic in ± 4 V range, the structure resistance the in the

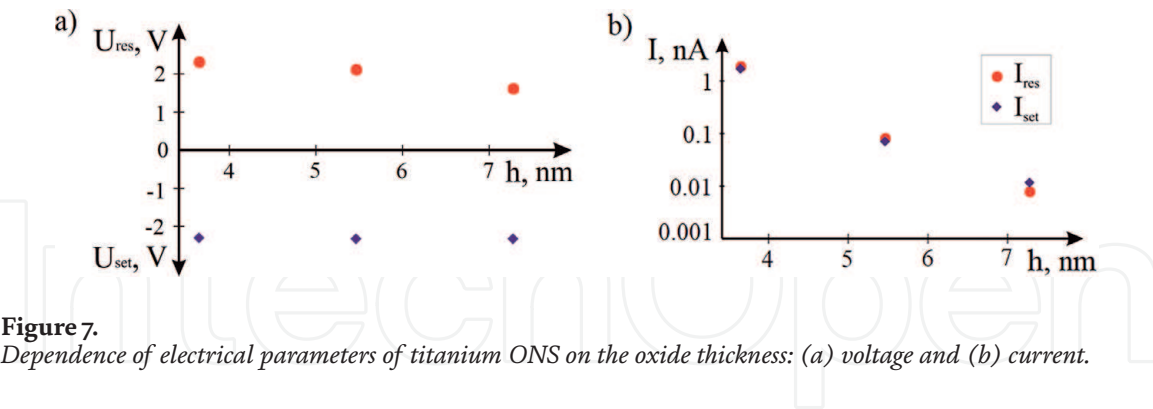


Figure 7.
Dependence of electrical parameters of titanium ONS on the oxide thickness: (a) voltage and (b) current.

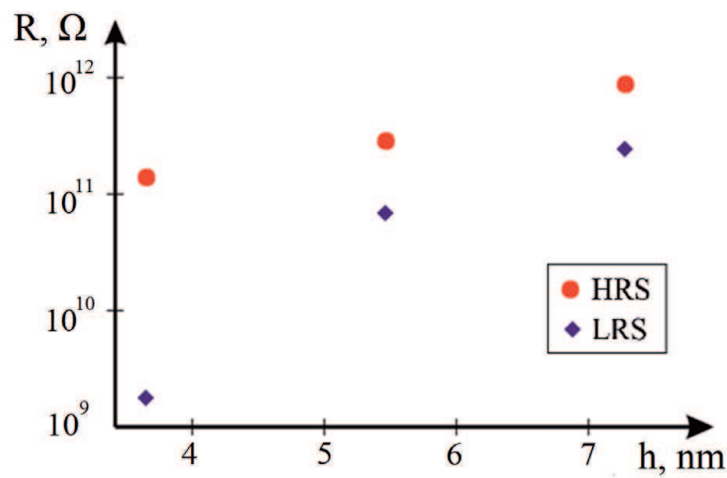


Figure 8.
Dependence of titanium ONS resistance on the thickness.

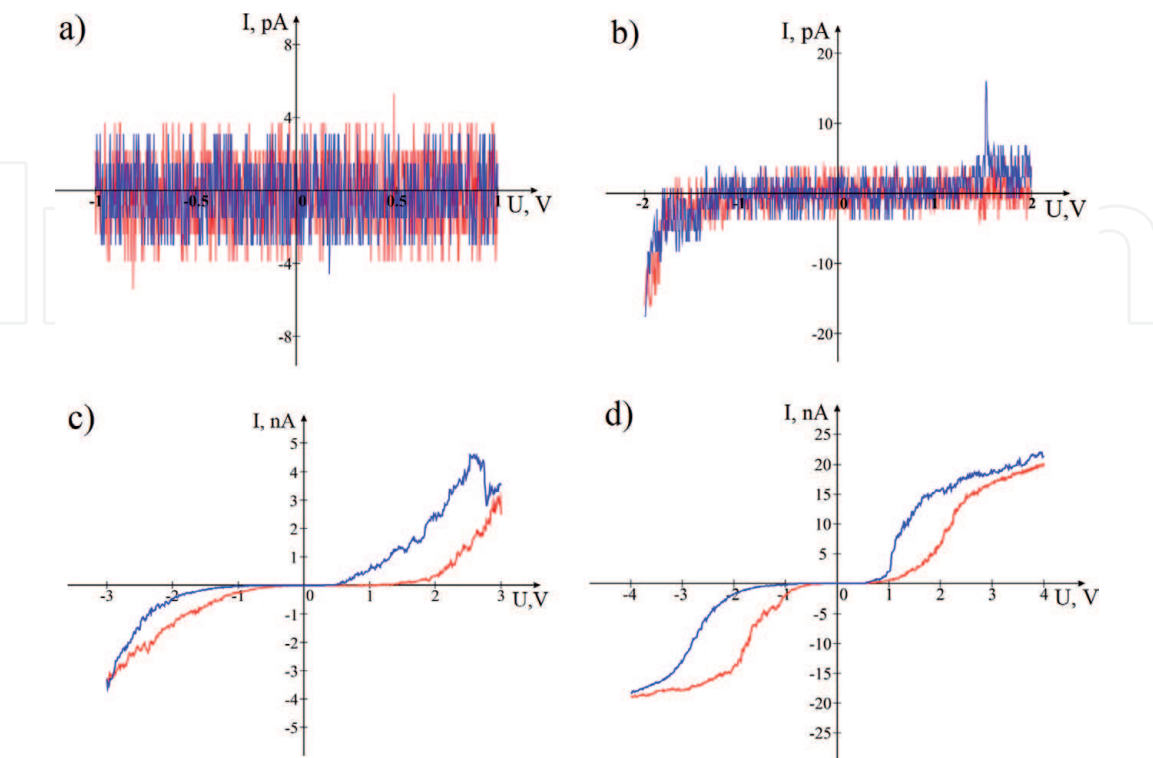


Figure 9.
Current-voltage characteristics of titanium ONS in the different voltage range: (a) ± 1 V; (b) ± 2 V; (c) ± 3 V; and (d) ± 4 V.

HRS state is $1.08 \times 10^9 \Omega$, and in the LRS state it is $0.14 \times 10^9 \Omega$, the resistance ratio in the HRS and LRS states is 7.5.

Such a memristor effect dependence on the titanium ONS thickness and the applied voltage pulses amplitude is explained by the electric field intensity influence in the oxide on the oxygen vacancies transfer in the oxide volume between the electrodes and the titanium ONS switching between high-resistance and low-resistance states.

3. Formation and investigation of memristor structures based on nanocrystalline ZnO thin films by atomic force microscopy

3.1 Investigation of resistive switching of nanocrystalline ZnO thin films

A resistive switching effect in thin oxide films is attractive for manufacturing of neuromorphic system, which offers significant advantages over classical computers, such as an effective processing of data recognition. ZnO is the one of the promising materials, which is widely used in electronic element developments, sensors, and microsystem technology. Also, ZnO demonstrates resistive switching, which has just one phase and is compatible with semiconductor technology. To fabricate ZnO-based neuromorphic system, it is necessary to study resistive switching in ZnO films and today there are insufficient experimental results about it.

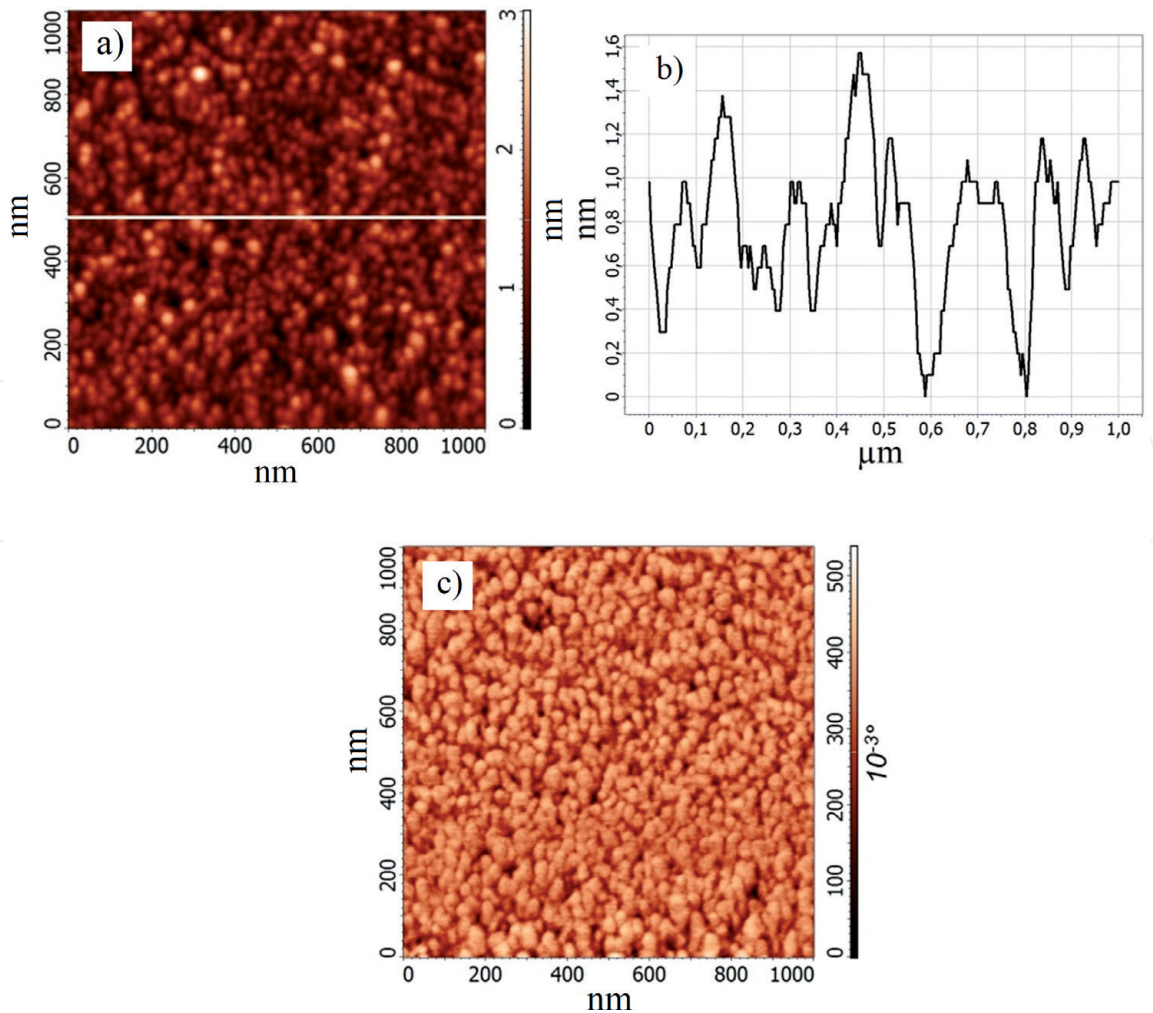


Figure 10.
ZnO film surface: (a) AFM-image; (b) AFM cross-sectional profile on (a); and (c) phase.

To investigate resistive switching $\text{Al}_2\text{O}_3/\text{ZnO}:\text{In}$ (42.1 ± 5.6 nm) as a wafer was used. ZnO thin films were grown using pulsed laser deposition under the following conditions: wafer temperature: 400°C , target-wafer distance: 50 mm, O_2 pressure: 1 mTorr, pulse energy: 300 ml. To provide electrical contact to the bottom ZnO:In electrode, ZnO films were deposited through a mask.

Electrical properties of obtained ZnO films were measured by Ecopia HMS-3000 equipment (Ecopia Co., Republic of Korea). Obtained ZnO films had electron concentration $8.4 \times 10^{19} \text{ cm}^{-3}$, electron mobility $12 \text{ cm}^2/\text{V}\cdot\text{s}$, and resistivity $5.2 \times 10^{-3} \Omega\cdot\text{cm}$.

AFM-images of the ZnO film surface were obtained in semi-contact mode using scanning probe microscope Solver 47 Pro (NT-MDT, Russia). The AFM-image processing was performed using Image Analysis software. **Figure 10** shows experimental investigations of ZnO film morphology. It is shown that ZnO film surface has a granular structure (**Figure 10a** and **c**) with 1.53 ± 0.27 nm roughness (**Figure 10b**). The ZnO film thickness was measured by ZnO/ZnO:In stair scanning, and was equaled 32.3 ± 7.2 nm.

Electrical measurements were taken using nanolaboratory Ntegra with W_2C probes. During the resistive switching investigation, ZnO:In film was grounded.

Current-voltage curves (CVC) were obtained from -3 to $+3$ V sweep for 15 cycles at the same point and for 15 cycles at different points on ZnO surface (**Figure 11a**). Based on the results obtained, resistance dependence on cycle number (uniformity test) and resistance dependence on number point were built (homogeneity test). It was shown R_{HRS} and R_{LRS} were equaled to $0.68 \pm 0.07 \text{ G}\Omega$ and $0.11 \pm 0.04 \text{ G}\Omega$,

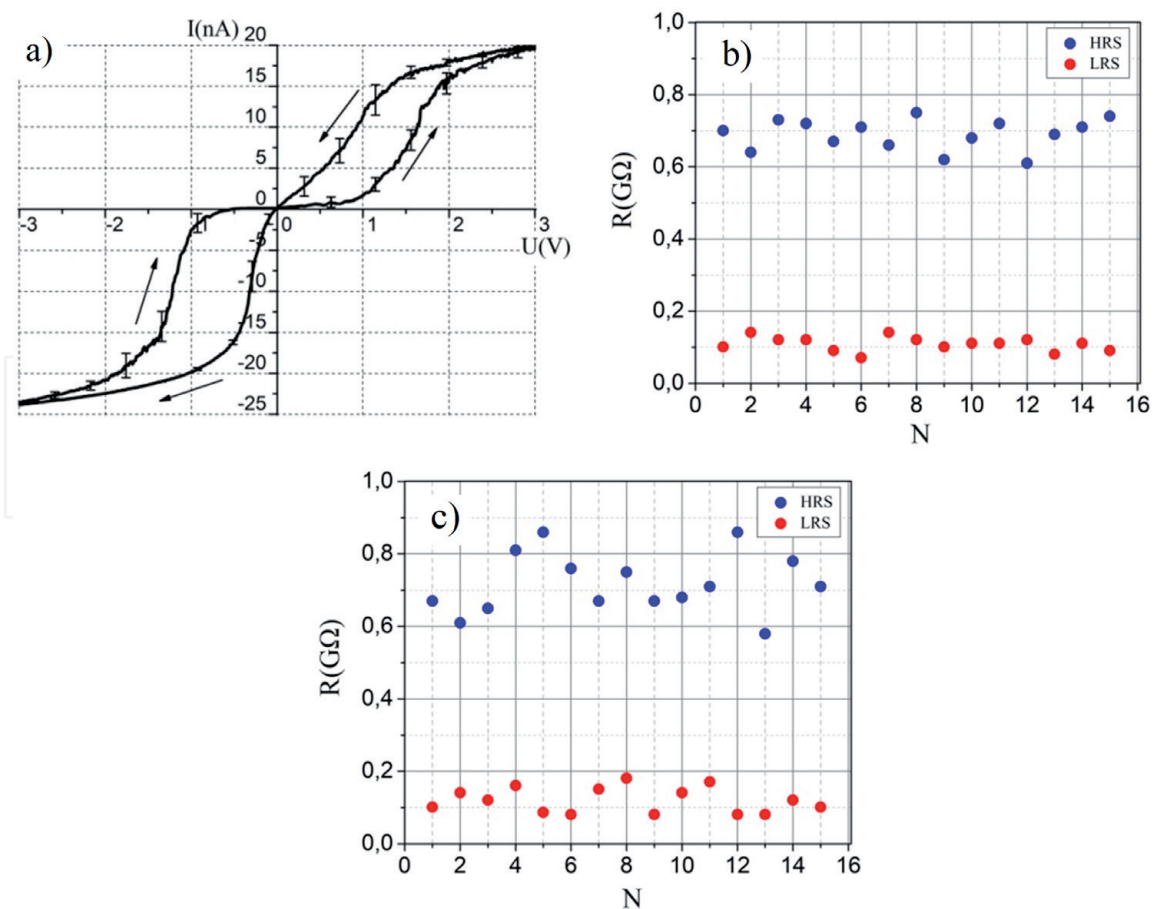


Figure 11. Investigation of resistive switching in ZnO film: (a) current-voltage characteristic; (b) uniformity; and (c) variability.

respectively at the same point on ZnO surface. At different points, R_{HRS} and R_{LRS} were equaled to $0.75 \pm 0.13 \text{ G}\Omega$ and $0.12 \pm 0.06 \text{ G}\Omega$. R_{HRS}/R_{LRS} was equaled to 9.05 ± 5.65 at 0.7 V. Resistance dispersion during uniformity test was more than resistance dispersion during homogeneity test that can be explained by a granular structure of ZnO film.

Time stability of resistive switching in ZnO was implemented using Ntegra in two stages. On the first stage, charge structure was formed on the ZnO surface at +5 V (Figure 12a). On the second stage, charged structure was scanned in Kelvin mode in the interval from 5 to 30 minutes with a step 5 minute (Figure 12b and c). It was shown that voltage decreased from 266 ± 17 to $68 \pm 7 \text{ mV}$ in 30 minutes (Figure 12a).

3.2 Investigation of scratching probe nanolithography regimes for memristor structure formation

Resistive switching element manufacturing is associated with the development and research of the formation processes of structures with a nanometer resolution. Existing lithographic methods of semiconductor technologies are approaching the limit of their resolution, characterized by a high degree of complexity and cost of equipment. Therefore, there is a need for research and development of new methods, the use of which will allow the creation of nanostructures of resistive switching elements, including at the prototyping stage. A promising method for the formation of nanoscale structures that can be used to create resistive switching elements is nanoimprint lithography based on the use of special dies and films of polymeric materials. A type of nanoimprint lithography is scratching probe nanolithography

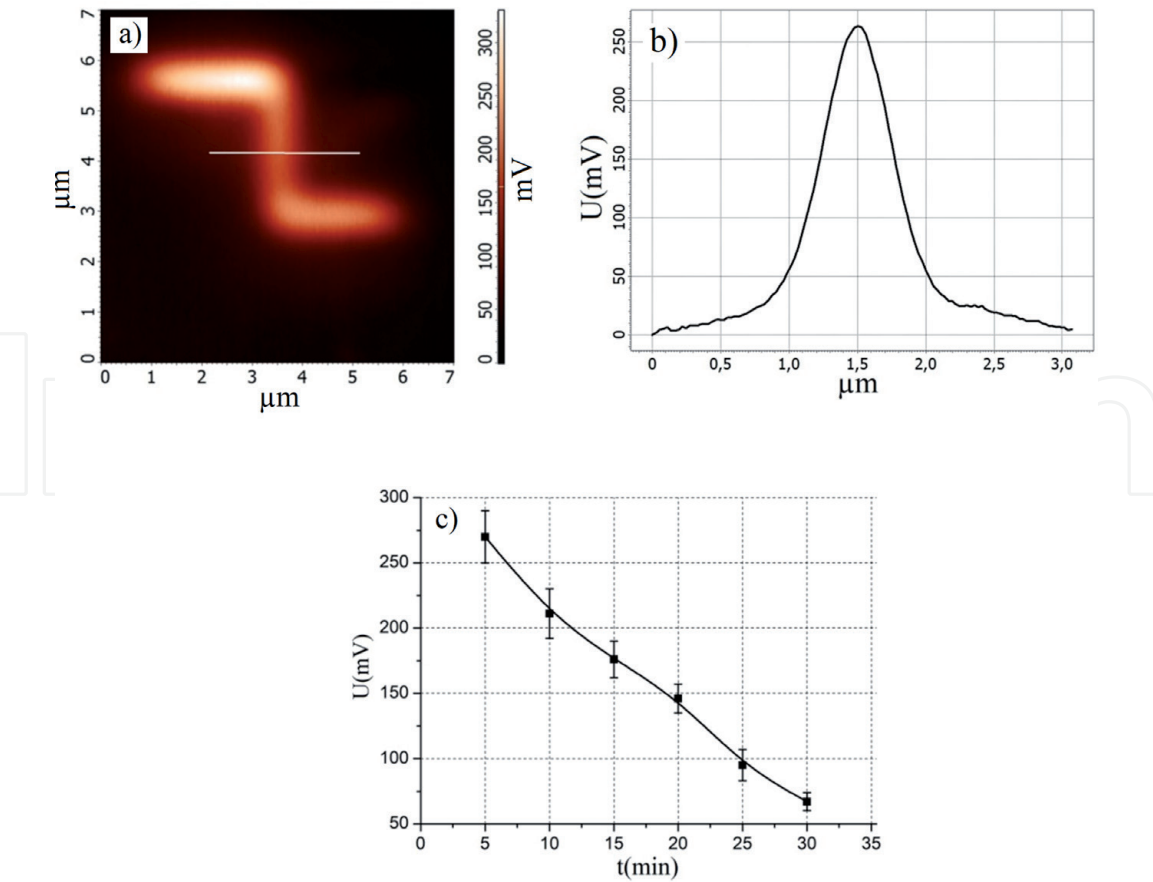


Figure 12. Investigation of ZnO film surface charge: (a) Kelvin mode image of charged structure; (b) AFM cross-sectional profile on (a); and (c) time dependence of voltage.

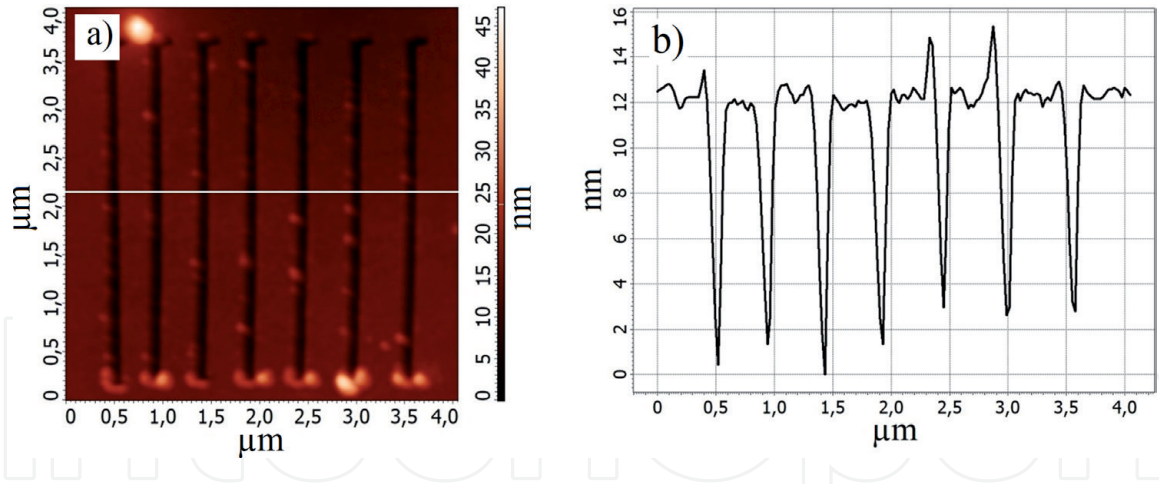


Figure 13. Profiled nanostructures on photoresist surface: (a) AFM-image; and (b) AFM cross-sectional profile on (a).

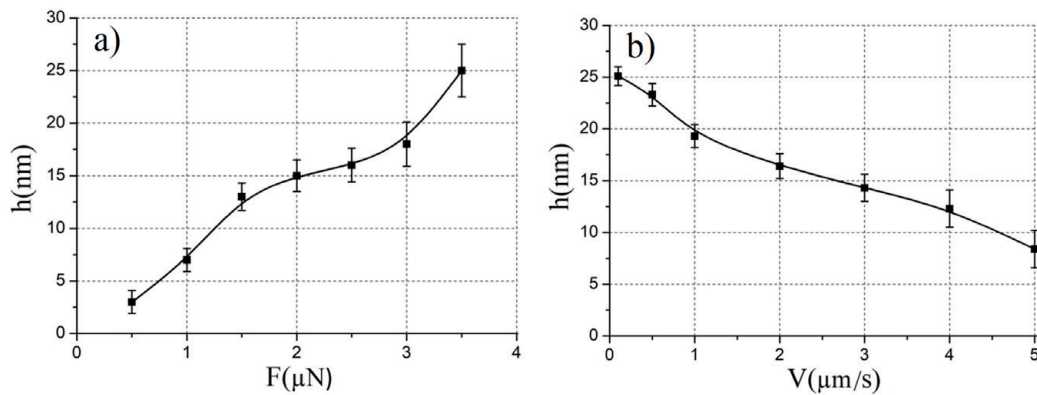


Figure 14. Investigation of scratching probe nanolithography regimes: (a) force of depth dependence; (b) velocity of depth dependence.

(SPN), which allows using the tip of an atomic force microscope probe to form profiled nano-sized structures in polymer films. It was decided to use photoresist FP-383 as polymer film, because it is cheaper and has longer shelf life compared to other types of polymer films.

The solution of photoresist/thinner (FP-383/RPF383F) at volume ratio of 1:10 was transferred onto Si substrate using the centrifugal method at the rotation speed of a Laurell WS-400B-6NPP centrifuge at 5000 rpm. After the deposition of the film, the photoresist/thinner film was dried at a temperature of 90°C for 25 minutes. Thickness of the photoresist/thinner film was equaled to 32.1 ± 4.7 nm.

Scratching probe nanolithography on the photoresist/thinner film was performed using a Solver P47 Pro scanning probe microscope. Indentation was performed by applying an AFM probe to the surface of a FP-383 film with a fixed clamping force (the Set Point parameter in the AFM control program). Thus, arrays of the seven profiled lines-grooves were formed at different nanoindentation forces (Figure 13).

Analysis of the results obtained showed that nanoindentation force increase from 0.5 to $3.5 \mu\text{N}$ leads to nanostructure-groove depth increase from 2.7 ± 0.8 to 25.31 ± 2.11 nm (Figure 14a), tip velocity increase from 0.1 to $5 \mu\text{m/s}$ leads to nanostructure-groove depth decrease from 25.10 ± 1.2 to 8.87 ± 1.34 nm (Figure 14b).

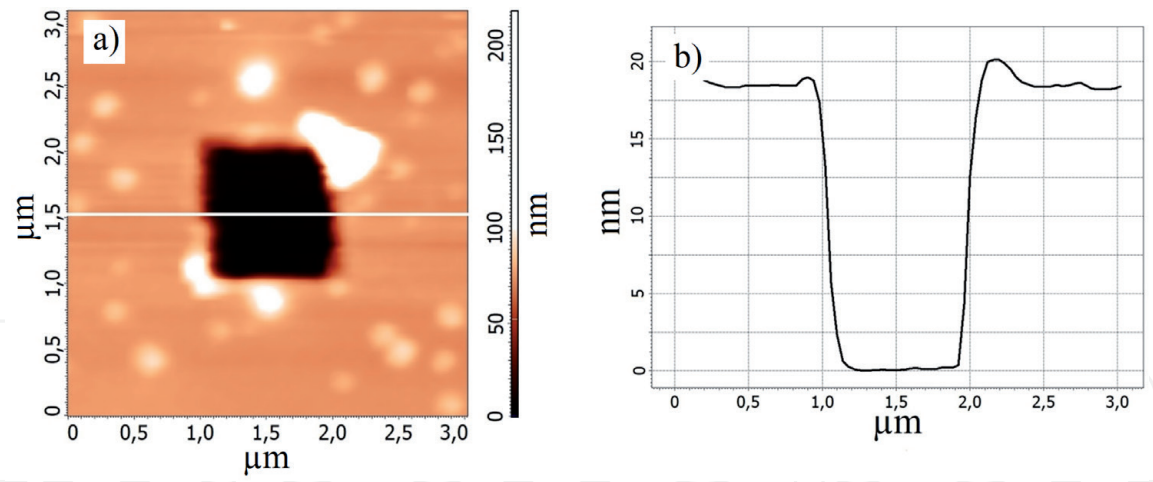


Figure 15.
Profiled nanostructure on FP-383 film surface: (a) AFM-image; and (b) AFM cross-sectional profile on (a).

The nonlinearity of the dependences obtained can be explained by the inhomogeneity of the viscoelastic properties of the FP-383 film. It should also be noted that the nature of the contact interaction between the probe and the film is complex and is largely determined by the elastic forces.

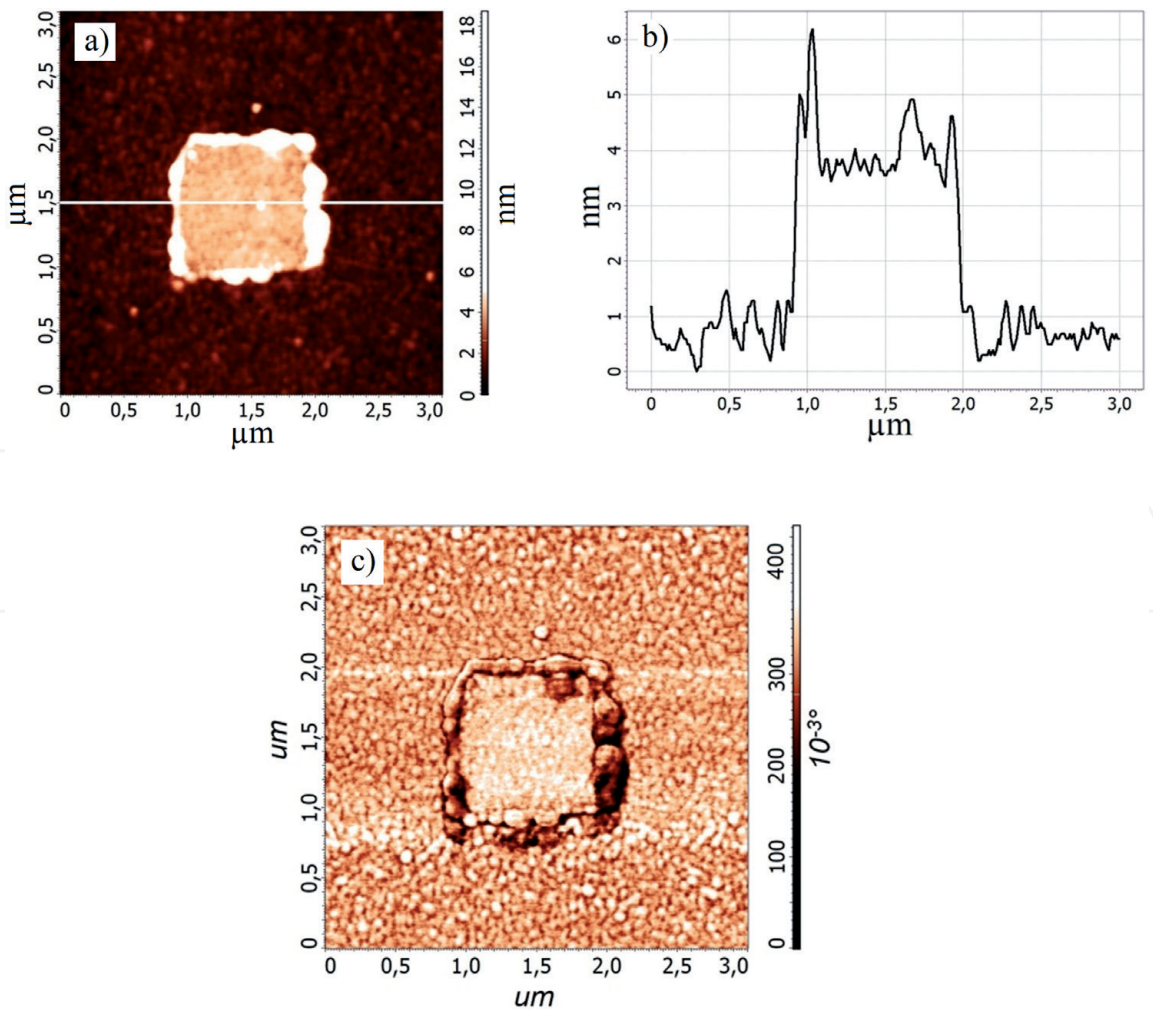


Figure 16.
Resistive switching $\text{Al}_2\text{O}_3/\text{ZnO:In}/\text{ZnO}/\text{Ti}/\text{W}_2\text{C}$ memristor structure: (a) AFM-image; (b) AFM cross-sectional profile on (a); and (c) phase.

3.3 Fabrication and investigation of resistive switching of memristor structures based on nanocrystalline ZnO thin films

To fabricate memristor structure, photoresist FP-383 thin film with thickness 21.4 ± 3.1 nm was formed on $\text{Al}_2\text{O}_3/\text{ZnO}:\text{In}/\text{ZnO}$ substrate. Then squared nanostructure-groove was formed on FP-383 film surface using scratching probe nanolithography at nanoindentation force $3.18 \mu\text{N}$ (**Figure 15**). Thin Ti film was deposited using BOC Edwards Auto 500 system. After that lift-off process was applied using dimethylformamide. AFM-image of the $\text{Al}_2\text{O}_3/\text{ZnO}:\text{In}/\text{ZnO}/\text{Ti}$ resistive switching structure obtained is shown in **Figure 16**. Analysis of the result obtained showed that Ti film thickness was equaled to 4.1 ± 0.3 nm (**Figure 16b**). Ripped edges of Ti structures are result of lift-off process.

Figure 17 shows current-voltage characteristic of $\text{Al}_2\text{O}_3/\text{ZnO}:\text{In}/\text{ZnO}/\text{Ti}/\text{W}_2\text{C}$ structure at -4 to $+4$ voltage sweep. It was shown that $\text{Al}_2\text{O}_3/\text{ZnO}:\text{In}/\text{ZnO}/\text{Ti}/\text{W}_2\text{C}$ structure has nonlinear, bipolar behavior when the electric potential gradient is the dominant parameter of resistive switching.

Investigation of resistive switching of $\text{Al}_2\text{O}_3/\text{ZnO}:\text{In}/\text{ZnO}/\text{Ti}/\text{W}_2\text{C}$ structure in the single point (uniformity test) shown that R_{HRS} was 8.23 ± 1.93 G Ω and R_{LRS} was 0.11 ± 0.06 G Ω (**Figure 17b**). At different points, R_{HRS} and R_{LRS} were equaled 7.65 ± 2.83 G Ω and 0.18 ± 0.11 G Ω , respectively (**Figure 17c**). It was shown, that $R_{\text{HRS}}/R_{\text{LRS}}$ coefficient was equaled 135.31 ± 44.38 at 0.7 V.

In the end, it was shown that the use of Ti film allowed to increase $R_{\text{HRS}}/R_{\text{LRS}}$ coefficient from 9.05 ± 5.65 to 135.31 ± 44.38 and to decrease the resistance dispersion of resistance switching (**Figures 11 and 17**). It can be explained by exception for the influence of air oxygen in $\text{Al}_2\text{O}_3/\text{ZnO}:\text{In}/\text{ZnO}/\text{Ti}$ structure that significantly worsens the resistive switching.

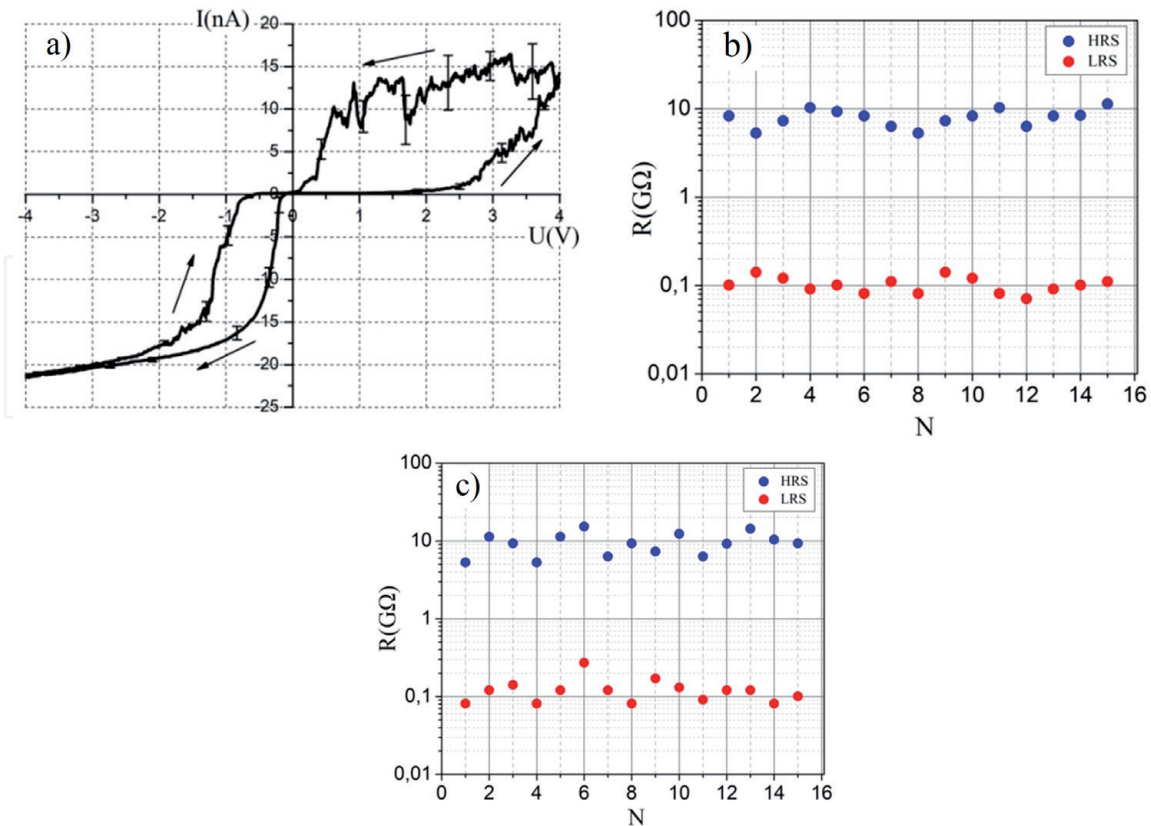


Figure 17.

Investigation of resistive switching in $\text{Al}_2\text{O}_3/\text{ZnO}:\text{In}/\text{ZnO}/\text{Ti}/\text{W}_2\text{C}$ structure: (a) current-voltage characteristic; (b) uniformity; and (c) homogeneity.

4. Investigation of resistive switching in vertically aligned carbon nanotubes using scanning tunnel microscopy

4.1 Influence of voltage pulses amplitude on resistive switching of strained carbon nanotubes

The dependence of the resistive switching of a vertically aligned carbon nanotube on the voltage pulse amplitude was studied using the STM spectroscopy using the probe nanolaboratory Ntegra. **Figure 18** shows the current-voltage characteristics of a strained carbon nanotube, obtained by applying a series of voltage sawtooth pulses with amplitude of 1–8 V, duration of 1 second, and tunnel gap of 1 nm. The diameter of a VA CNT of the investigated array was 95 ± 5 nm, length 2.3 ± 0.2 μm , and density of nanotubes in the array was $18 \mu\text{m}^{-2}$. It should be noted that the current-voltage characteristics are represented in the range from 0 to 50 nA, which relates to the peculiarities of the measuring system of the scanning tunneling microscope.

The measurement results showed that resistive switching of the VA CNT does not occur when the applied voltage amplitude is less than 2 V (**Figure 18a**). This is due to the insufficient value of the external electric field for the formation of a low-resistance state in the nanotube [28]. The reproducible resistive switching was observed with a further increase in amplitude to 4 V and more (**Figure 18b–d**).

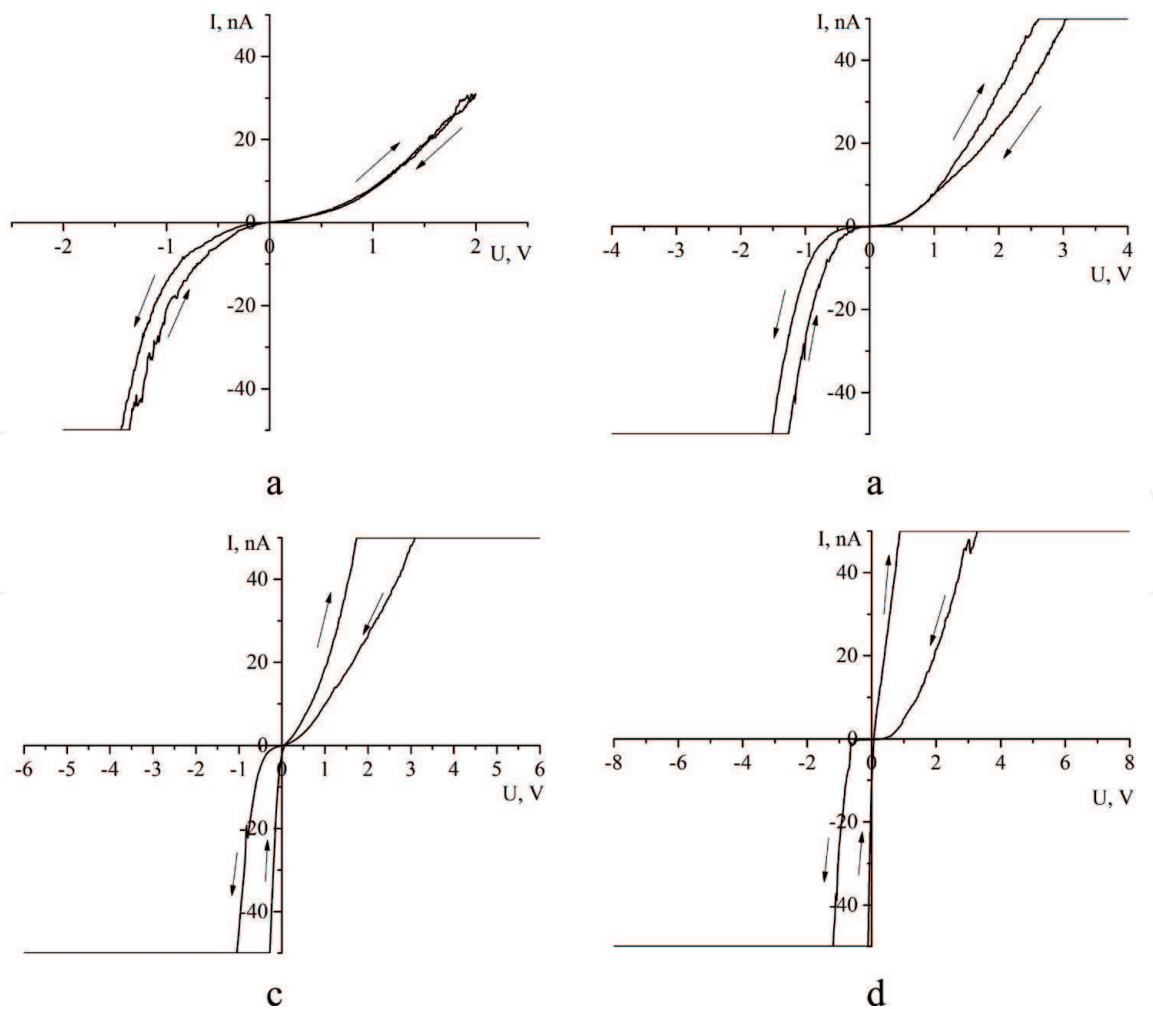


Figure 18.
CVCs of VA CNT upon application of a series of sawtooth voltage pulses with amplitude: (a) 2 V; (b) 4 V; (c) 6 V; and (d) 8 V.

The R_{HRS}/R_{LRS} ratio increased from 1 to 52 with an increase in the amplitude U from 1 to 8 V. This dependence is explained by the fact that the nanotube had the same resistance values of R_{HRS} , while the resistance of its low resistance state decreased inversely to the increase in the applied voltage amplitude due to the compensation of the internal electric field arising during deformation of the VA CNT with an external electric field [28].

It should be noted that the values of R_{HRS} and R_{LRS} of the VA CNT are 2–3 times lower at $U < 0$ than at $U > 0$. It is due to the fact that associated with the occurrence of a piezoelectric charge, internal field of the nanotube [33, 34] is co-directed with an external electric field, and accordingly, reduces the resistance of the VA CNT when a negative voltage is applied and is oppositely directed and increases the total resistance of the VA CNT when a positive voltage is applied.

4.2 Influence of deformation on resistive switching of strained carbon nanotubes

The studies of the influence of deformation on resistive switching of a VA CNT were performed by the STM spectroscopy with a tunneling gap $d = 0.2, 0.5, 1$, and 2 nm. Controlled elastic deformation of VA CNT was formed on the basis of the previously developed technique [32] and was equal to the tunnel gap. The value d was determined on the basis of current-height characteristics and was controlled using the STM feedback system. **Figure 19** shows the experimental current-voltage characteristics obtained by applying voltage sawtooth pulses with amplitudes of 4 and 8 V.

Analysis of the obtained CVCs showed that at $U = 4$ V, the R_{LRS} value initially decreased and increased again at $\Delta L = d = 2$ nm (**Figure 19a**). This is due to the fact that the magnitude of the external electric field was not enough to compensate the internal electric field of the nanotube at a deformation of 2 nm. This effect disappeared as the voltage amplitude increased to $U = 8$ V due to an increase in the external electric field (**Figure 19b**). The values of R_{HRS} and R_{LRS} of the VA CNT decreased with increasing deformation (**Figure 19b**). The decrease in the of R_{HRS} and R_{LRS} of the VA CNT is due to the increase in the initial deformation $\Delta L \approx d$ and the corresponding value of the piezoelectric charge, and is consistent with the mechanism of memristive switching of VA CNT [28].

It was also shown that the R_{HRS}/R_{LRS} ratio of the VA CNT does not depend on the deformation value and is determined by the value of the applied voltage: the $R_{HRS}/R_{LRS} = 2-3$ at $U = 4$ V (**Figure 19a**) and the $R_{HRS}/R_{LRS} > 50$ at $U = 8$ V (**Figure 19b**).

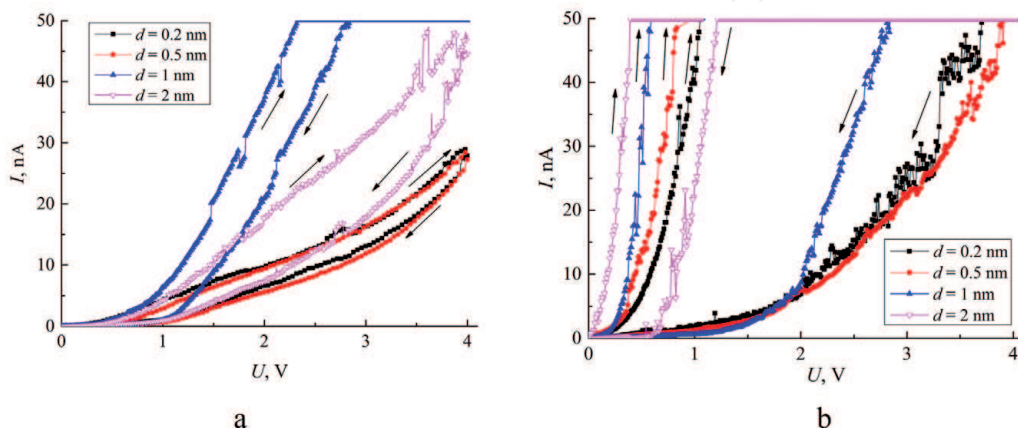


Figure 19. CVCs of VA CNT at various values of deformation $\Delta L \approx d$ and at voltage sawtooth pulses amplitude: (a) 4 V; and (b) 8 V.

5. Conclusion

Thus, application of scanning probe microscopy techniques for fabrication and determination of electrical parameters of memristor structures based on vertically aligned carbon nanotubes, titanium oxide nanostructures, and nanocrystalline ZnO thin films was presented. It is shown that titanium oxide nanostructures obtained by local anodic oxidation have a memristor effect without additional electroforming. The regularities of the manifestation of the memristor properties of oxide nanoscale structures of titanium are established, and the effect of the thickness of oxide nanoscale structures and the amplitude of applied voltage pulses on the displayed memristor effect in them is shown. It was found that the oxide nanoscale structures of titanium with a thickness of 1.6 nm have a resistance ratio in the high resistance to low resistance equal to 79.4. By using scratching probe nanolithography was made memristor structure based on nanocrystalline ZnO thin film obtained by pulsed laser deposition. The results can be used for micro- and nano-electronic elements manufacturing, as well as memristor structures, ReRAM elements using probe nanotechnologies, and for metal oxide and VA CNT-based neuromorphic system fabrication. The results of the study of resistive switching of vertical aligned carbon nanotubes using scanning tunneling microscopy are presented.

The results were obtained using the equipment of Research and Education Center and the Center for collective use “Nanotechnologies” of Southern Federal University.

Acknowledgements

This work was financially supported by Russian Foundation for Basic Research (projects No. 16-29-14023 ofi_m, 18-37-00299 mol_a) and internal grant of the Southern Federal University (project No. VnGr-07/2017-26).

Conflict of interest


The authors declare no conflict of interest.

Author details

Vladimir A. Smirnov*, Marina V. Il'ina, Vadim I. Avilov, Roman V. Tominov,
Oleg I. Il'in and Oleg A. Ageev
Southern Federal University, Institute of Nanotechnologies, Electronics
and Electronic Equipment Engineering, Taganrog, Russia

*Address all correspondence to: vasmirnov@sfedu.ru

IntechOpen

© 2019 The Author(s). Licensee IntechOpen. This chapter is distributed under the terms of the Creative Commons Attribution License (<http://creativecommons.org/licenses/by/3.0>), which permits unrestricted use, distribution, and reproduction in any medium, provided the original work is properly cited. 

References

- [1] Zidan M, Strachan J, Lu W. The future of electronics based on memristive systems. *Nature Electronics*. 2018;**1**:22-29. DOI: 10.1038/s41928-017-0006-8
- [2] Hong X, Loy D, Dananjaya P, Tan F, Ng C, Lew W. Oxide-based RRAM materials for neuromorphic computing. *Journal of Materials Science*. 2018;**53**:8720-8746. DOI: 10.1007/s10853-018-2134-6
- [3] Wang L, Zhang W, Chen Y, Cao Y, Li A, Wu D. Synaptic plasticity and learning behaviors mimicked in single inorganic synapses of Pt/HfO_x/ZnO_x/TiN memristive system. *Nanoscale Research Letters*. 2017;**12**:65. DOI: 10.1186/s11671-017-1847-9
- [4] Abbas H, Abbas Y, Truong S, Min K, Park M, Cho J, et al. A memristor crossbar array of titanium oxide for non-volatile memory and neuromorphic applications. *Semiconductor Science and Technology*. 2017;**32**:201732-065014. DOI: 10.1088/1361-6641/aa6a3a
- [5] Bai Y, Wu H, Wu R, Zhang Y, Deng N, Yu Z, et al. Study of multi-level characteristics for 3D vertical resistive switching memory. *Scientific Reports*. 2014;**4**:5780. DOI: 10.1038/srep05780
- [6] Meena J, Sze S, Chand U, Tseng T. Overview of emerging nonvolatile memory technologies. *Nanoscale Research Letters*. 2014;**9**:526. DOI: 10.1186/1556-276X-9-526
- [7] Chen A. A review of emerging non-volatile memory (NVM) technologies and applications. *Solid-State Electronics*. 2016;**125**:25-38. DOI: 10.1016/j.sse.2016.07.006
- [8] Chang T, Chang K, Tsai T, Chu T, Sze S. Resistance random access memory. *Materials Today*. 2016;**19**:254-264. DOI: 10.1016/j.mattod.2015.11.009
- [9] Pan F, Gao S, Chen C, Song C, Zeng F. Recent progress in resistive random-access memories: Materials, switching mechanisms, and performance. *Materials Science and Engineering R*. 2014;**83**:1-59. DOI: 10.1016/j.mser.2014.06.002
- [10] Ha S, Ramanathan S. Adaptive oxide electronics: A review. *Journal of Applied Physics*. 2011;**110**:14. DOI: 10.1063/1.3640806
- [11] Siles P, Archanjo B, Baptista D, Pimentel V, Joshua J. Nanoscale lateral switchable rectifiers fabricated by local anodic oxidation. *Journal of Applied Physics*. 2011;**110**:024511. DOI: 10.1063/1.3609065
- [12] Avilov V, Ageev O, Kolomiitsev A, Konoplev B, Smirnov V, Tsukanova O. Formation of a memristor matrix based on titanium oxide and investigation by probe-nanotechnology methods. *Semiconductors*. 2014;**48**:1757-1762. DOI: 10.1134/S1063782614130028
- [13] Avilov V, Polupanov N, Tominov R, Smirnov V, Ageev O. Scanning probe nanolithography of resistive memory element based on titanium oxide memristor structures. *IOP Conference Series: Materials Science and Engineering*. 2017;**256**:012001. DOI: 10.1088/1757-899X/256/1/012001
- [14] Tsai J, Hsu C, Hsu C, Yang C, Lin T. Fabrication of resistive random-access memory by atomic force microscope local anodic oxidation. *NANO: Brief Reports and Reviews*. 2015;**10**:1550028. DOI: 10.1142/S1793292015500289
- [15] Polyakova V, Smirnov V, Ageev O. A study of nanoscale profiling modes of a silicon surface via local anodic oxidation. *Nanotechnologies in Russia*. 2018;**13**:84-89. DOI: 10.1134/S1995078018010111

- [16] Avilov V, Ageev O, Konoplev B, Smirnov V, Solodovnik M, Tsukanova O. Study of the phase composition of nanostructures produced by the local anodic oxidation of titanium films. *Semiconductors*. 2016;**50**:601-606. DOI: 10.1134/S1063782616050043
- [17] Avilov V, Ageev O, Blinov Y, Konoplev B, Polyakov V, Smirnov V, et al. Simulation of the formation of nanosize oxide structures by local anode oxidation of the metal surface. *Technical Physics*. 2015;**60**:717-723. DOI: 10.1134/S1063784215050023
- [18] Avilov V, Ageev O, Smirnov V, Solodovnik M, Tsukanova O. Studying the modes of nanodimensional surface profiling of gallium arsenide epitaxial structures by local anodic oxidation. *Nanotechnologies in Russia*. 2015;**10**:214-219. DOI: 10.1134/S1995078015020032
- [19] Smirnov V. Chapter: Nanolithography by local anodic oxidation of thin titanium film. In book: *Piezoelectrics and Nanomaterials: Fundamentals, Developments and Applications*. Nova science, 2015. p. 85-103. ISBN: 978-163483351-6;978-163483319-6
- [20] Ryu Y, Garcia R. Advanced oxidation scanning probe lithography. *Nanotechnology*. 2017;**28**:142003. DOI: 10.1088/1361-6528/aa5651
- [21] Tominov R, Smirnov V, Chernenko N, Ageev O. Study of the regimes of scratching probe nanolithography. *Nanotechnologies in Russia*. 2017;**12**:650-657. DOI: 10.1134/S1995078017060131
- [22] Tominov R, Smirnov V, Avilov V, Fedotov A, Klimin V, Chernenko N. Formation of ZnO memristor structures by scratching probe nanolithography. *IOP Conference Series: Materials Science and Engineering*. 2018;**443**:012036. DOI: 10.1088/1757-899X/443/1/012036
- [23] Smirnov V, Tominov R, Alyabeva N, Ilina M, Polyakova V, Bykov A, et al. Atomic force microscopy measurement of the resistivity of semiconductors. *Technical Physics*. 2018;**63**:1236-1241. DOI: 10.1134/S1063784218080182
- [24] Smirnov V, Shandyba N, Panchenko I, Tominov R, Pelipenko M, Zamburg E, et al. Size effect on memristive properties of nanocrystalline ZnO film for resistive synaptic devices. *Journal of Physics: Conference Series*. 2018;**1124**:081036. DOI: 10.1088/1742-6596/1124/8/081036
- [25] Ageev O, Konoplev B, Rubashkina M, Rukomoikin A, Smirnov V, Solodovnik M. Studying the effect of geometric parameters of oriented GaAs nanowhiskers on Young's modulus using atomic force microscopy. *Nanotechnologies in Russia*. 2013;**8**:23-28. DOI: 10.1134/S1995078013010023
- [26] Il'ina M, Il'in O, Smirnov V, Blinov Y, Konoplev B, Ageev O. Scanning probe techniques for characterization of vertically aligned carbon nanotubes. In: *Atomic-force microscopy and its applications*. IntechOpen; 2018. DOI: 10.5772/intechopen.78061
- [27] Choi W, Bae E, Kang D, Chae S, Cheong B, Ko J, et al. Aligned carbon nanotubes for nanoelectronics. *Nanotechnology*. 2004;**15**:512-516. DOI: 10.1088/0957-4484/15/10/003
- [28] Il'ina M, Il'in O, Blinov Y, Smirnov V, Kolomiitsev A, Fedotov A, et al. Memristive switching mechanism of vertically aligned carbon nanotubes. *Carbon*. 2017;**123**:514-524. DOI: 10.1016/j.carbon.2017.07.090
- [29] Chen H, Roy A, Baek J, Zhu L, Qu J, Dai L. Controlled growth and modification of vertically-aligned carbon nanotubes for multifunctional applications. *Material Science Engineering Reports*. 2010;**70**:63-91. DOI: 10.1016/j.mser.2010.06.003

- [30] Ageev O, Balakirev S, Bykov A, Gusev E, Fedotov A, Jityaeva J, et al. Development of new metamaterials for advanced element base of micro- and nanoelectronics, and microsystem devices. In: *Advanced Materials-Manufacturing, Physics, Mechanics and Applications*. Switzerland: Springer International Publishing; 2016. pp. 563-580. DOI: 10.1007/978-3-319-26324-3_40
- [31] Ageev O, Blinov Y, Il'ina M, Il'in O, Smirnov V. Modeling and experimental study of resistive switching in vertically aligned carbon nanotubes. *Journal of Physics: Conference Series*. 2016;**741**:12168. DOI: 10.1088/1742-6596/741/1/012168
- [32] Il'ina M, Il'in O, Blinov Y, Smirnov V, Ageev O. Nonuniform elastic strain and Memristive effect in aligned carbon nanotubes. *Technical Physics*. 2018;**63**:1672-1677. DOI: 10.1134/S1063784218110129
- [33] Il'ina M, Il'in O, Blinov Y, Konshin A, Konoplev B, Ageev O. Piezoelectric response of multi-walled carbon nanotubes. *Materials (Basel)*. 2018;**11**:638. DOI: 10.3390/ma11040638
- [34] Il'ina M, Blinov Y, Il'in O, Rudyk N, Ageev O. Piezoelectric effect in non-uniform strained carbon nanotubes. *IOP Conference Series Material Science Engineering*. 2017;**256**:12024. DOI: 10.1088/1757-899X/256/1/012024